Original Article

Hydrochemical characterization and irrigation suitability of the Ganges Brahmaputra River System: review and assessment

BISHWAKARMA Kiran[1,2] https://orcid.org/0000-0002-0947-4697; e-mail: kiranghatani2019@itpcas.ac.cn

WANG Guan-xing[1*] https://orcid.org/0000-0002-3946-609X; e-mail: wangguanxing@itpcas.ac.cn

ZHANG Fan[1] https://orcid.org/0000-0002-6714-9534; e-mail: zhangfan@itpcas.ac.cn

ADHIKARI Subash[3] https://orcid.org/0000-0003-1116-5161; e-mail: subasnir@gmail.com

KARKI Kabita[1,5] https://orcid.org/0000-0002-9307-4310; e-mail: kabita@itpcas.ac.cn

GHIMIRE Archana[2,4] https://orcid.org/0000-0002-3706-613X; e-mail: archkasyab@gmail.com

**Corresponding author*

1 State Key Laboratory of Tibetan Plateau Earth System, Resources and Environment (TPESRE), Chinese Academy of Sciences, Beijing 100101, China

2 University of Chinese Academy of Sciences, Beijing 100049, China

3 Provincial Policy and Planning Commission, Gandaki Province, Pokhara 33700, Nepal

4 Research Center for Eco-Environmental Sciences, Chinese Academy of Sciences, Beijing 100085, China

5 Department of Mines and Geology, Kathmandu 44618, Nepal

Citation: Bishwakarma K, Wang GX, Zhang F, et al. (2022) Hydrochemical characterization and irrigation suitability of the Ganges Brahmaputra River System: review and assessment. Journal of Mountain Science 19(2). https://doi.org/10.1007/s11629-021-6834-z

Abstract: The hydrochemical characterization and irrigation suitability assessment of the Ganges-Brahmaputra River System (GBRS) has immense importance for the livelihoods of people and ecosystem sustainability in the region. This study aims to assess the hydrochemical characteristics and evaluate the irrigation suitability of water in the GBRS by reviewing published literature of the major tributaries. The studied rivers were categorized into two groups namely Group-1 and Group-2 considering the similarities of climatic patterns, hydrochemical attributes, and drainage characteristics. The hydrochemistry of the river water was characterized by the Piper diagram, Gibbs plot, mixing plots, and ionic ratios. Furthermore, irrigation water qualities were evaluated by electrical conductivity (EC), sodium percentage (Na%), sodium adsorption ratio (SAR), magnesium hazard (MH), and Wilcox diagram. The results indicated that the hydrochemistry of the GBRS was slightly alkaline to alkaline (7.42–8.78) in nature. The average concentrations of most of the chemical attributes showed higher in Group-1, whereas the average concentrations of K^+ and NO_3^- were found higher in Group-2. The average concentration of the major ions followed the dominancy order $Ca^{2+} > Mg^{2+} > Na^+ > K^+$ for cations and $HCO_3^- > SO_4^{2-} > Cl^- > NO_3^-$ for anions in both groups. Gibbs plot and mixing plot indicated that carbonate rock weathering dominates the hydrochemical process, which was further confirmed by the Piper diagram and the ionic ratios. From the analyses of irrigational water quality, almost all the rivers (except Gomti River in terms of MH and Rangit River in terms of Na%) in the GBRS were found to be suitable based on EC, SAR, Na%, MH, and Wilcox diagram. Finally, the majority of river systems in the GBRS were characterized by carbonate dominated lithology and irrigational water quality is

Received: 08-Apr-2021
Revised: 23-Jul-2021
Accepted: 22-Aug-2021

mostly suitable for utilization. This study could be useful for water quality management in the glacial-fed Himalayan river under the context of global climate change.

Keywords: Ganges-Brahmaputra River System; Hydrochemical characterization; Major ions; Irrigation suitability assessment

1 Introduction

Hydrochemical characteristics in the river water have a key role in ecological and economical perspectives. The overall concentration of dissolved constituents in river water determines its suitability for domestic purposes (Salifu et al. 2017). The dissolved ions in water, mainly calcium (Ca^{2+}), magnesium (Mg^{2+}), sodium (Na^{+}), potassium (K^{+}), bicarbonate (HCO_3^-), carbonate (CO_3^-), sulfate (SO_4^{2-}), chloride (Cl^-), and nitrate (NO_3^-) are the most abundant dissolved constituents in the river water (Meybeck and Ragu 1997). The chemical characteristics of the river basin can reflect the natural and anthropogenic interferences in the catchment. For instance, the primary source of riverine Ca^{2+}, Mg^{2+}, SO_4^{2-}, and HCO_3^- is natural, whereas NH_4^+ and NO_3^- are induced from anthropogenic activities (Huang et al. 2008; Haidary et al. 2013).

The chemical signatures and factors controlling the river hydrochemistry of the world major rivers have been well documented from the 1980s considering the Amazon River (Stallard and Edmond, 1983), Ganges-Brahmaputra River (Sarin et al. 1989, 1992), Yellow River (Zhang et al. 1995), Nile River (Dekov et al. 1997), Indus River (Qaisar et al. 2018), Mississippi River (Sharif et al. 2008), Mekong River (Huang et al. 2009), Tigris River (Varol et al. 2013), Yangtze River (Huang et al. 2009; Jiang et al. 2015), and eleven major rivers originated in the Tibetan plateau (Qu et al. 2019). The natural hydrochemistry of surface water is primarily controlled by rock weathering, precipitation, and evaporation-crystallization (Gibbs 1970). Moreover, groundwater discharge and anthropogenic interferences also significantly influence the hydrochemical properties of surface water.

In general, the water quality is defined based on EC, TDS, major ions, organic matters, nutrients contain, and various dissolving trace elements in water and have a significant role to determine the quality of irrigation water. However, TDS, EC, and major ions have been broadly used as primary parameters for irrigation water quality assessment (Acharya et al. 2020). In fact, salinity and ion toxicity are notable complications in irrigation water (Zaman et al. 2018). A sufficient amount of water with a permissible limit of salinity and ion toxicity is essential for the proper growth of plants and soil permeability (Kumari 2017). The salinity hazard, magnesium hazard and sodium hazard are major types of salt problems in irrigation water. High salinity in irrigation water is toxic for the plants. For example, irrigation water with more than 60% sodium content may lead to a breakdown in the soil's physical properties. The excess Na% combining with carbonate may result in the formation of alkali soils (Fipps 1995). Similarly, the excessive concentration of Ca^{2+} and Mg^{2+} in irrigation water can alter the salinity, increase the pH of the soil, affect the permeability properties of the soil root zone, and reduce the availability of phosphorous nutrient (Al-Shammiri et al. 2005; Joshi et al. 2009; Singh et al. 2018).

The Ganges-Brahmaputra River System (GBRS) is one of the largest river systems in the world ranking first and fourth in terms of sediment transport and river discharge, respectively (Milliman and Meade 1983; Sarin et al. 1989) (Fig. 1). The origins of the Ganges and the Brahmaputra are both the mountains of the Himalaya, however, they have distinctly different paths before joining at Bay of Bengal (Subramanian and Ramanathan 1996). The mainstream of the Ganges originates from the Gangotri Glacier at Gomukh (30°36′ N; 79°04′ E) in the Garhwal Himalaya range (Vass et al. 2010) and it crosses the Great Lesser Himalaya southward before flowing down into the Indo-Gangetic Plain (IGP) (Kuehl et al. 2011). Brahmaputra (also known as the Yarlung Tsangpo in Tibet) originates from the Angsi Glacier (at 5300 m asl) located on the northern side of the Himalaya in Tibet, travels eastward through the northern slope of the Himalayas, transverse to the southward and enters into the nanga Parbat before mixed with Ganges (Das et al. 2016). Table 1 further elaborates the key information of the GBRS.

The river hydrochemistry of the GBRS was first introduced in the 1990s. The hydrochemistry of the GBRS was dominated by carbonate and silicate weathering, while Ca^{2+}, Mg^{2+} and HCO_3^- accounted for more than 80% of the total ions (Sarin et al. 1989).

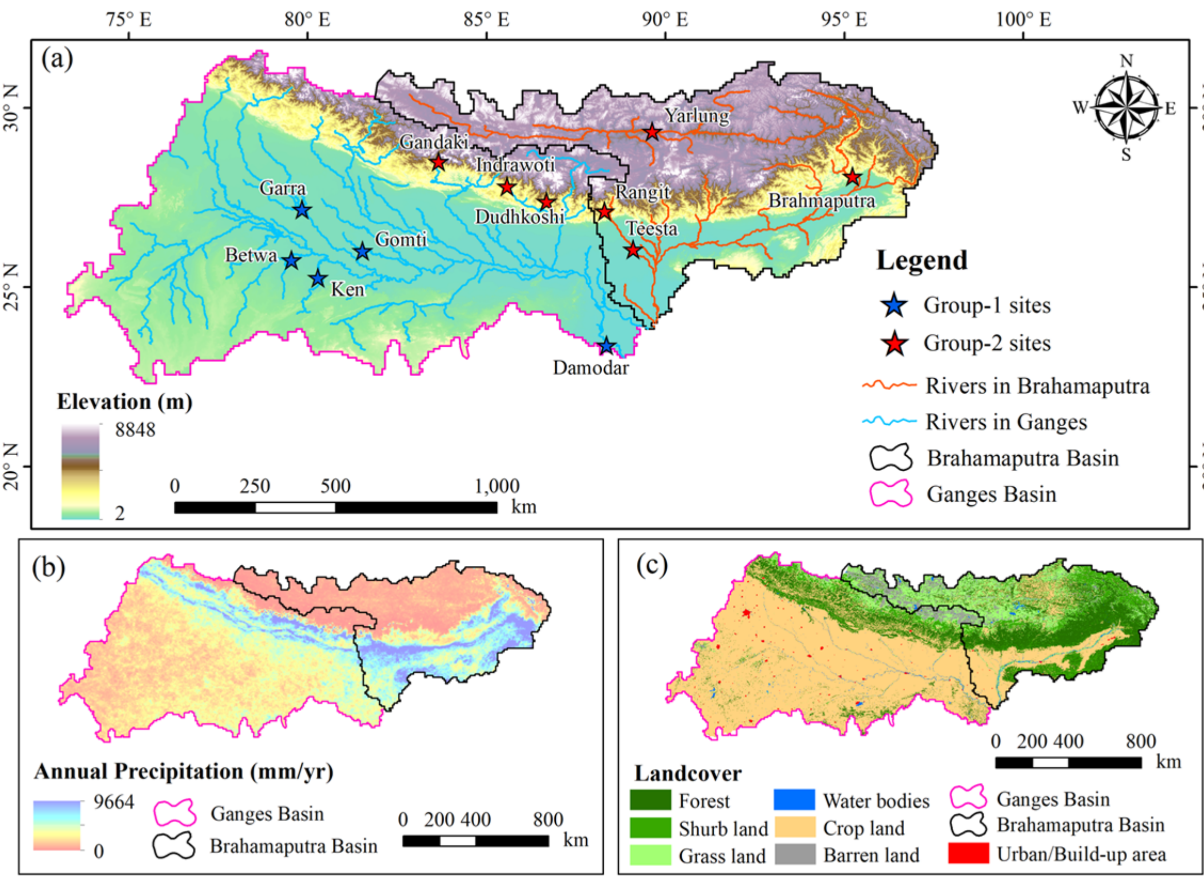

Fig. 1 Study area. (a) Basin map of the GBRS, (b) precipitation distribution pattern of the GBRS, and (c) land cover map of the GBRS. (Average Annual Precipitation during 1998-2009: http://www.geog.ucsb.edu/~bodo/TRMM/; land cover in 2019: https://ladsweb.modaps.eosdis.nasa.gov/search/order/1/MCD12Q1--6).

Table 1 FAO guidelines of pH, EC and major ions for irrigation water quality

Parameter	pH	EC	Ca^{2+}	Mg^{2+}	Na^{+}	K^{+}	Cl^{-}	SO_4^{2-}	NO_3^{-}	HCO_3^{-}
Permissible Limit	8.5	3000	19.96	4.938	39.98	0.51	29.98	19.97	0.16	10

Notes: Values were expressed in meq/L except pH and EC (μS/cm).

The tributaries of the Ganges like Ramganga, Gomti, Gandaki, and the Yamuna have been intensively studied (Sarin et al. 1989; Rai et al. 2010; Avtar et al. 2011; Seth et al. 2016; Pant et al. 2018) till date and revealed the dominancy of Ca^{2+}, Mg^{2+} and HCO_3^-, while the concentration of Na^{+}+K^{+} in tributaries of the lower stretches of the GBRS was relatively higher than the Himalaya level. The river water quality of the GBRS is reducing due to the intense stresses of anthropic disturbances surrounding the drainage area. The continuous decline of surface water quality of the GBRS is now a serious issue for the sustainable management of freshwater resources.

The study of hydrochemical characterization and assessment in the GBRS water is important in deciding its quality and valuable contribution to the study of the temporal and spatial changes in water resources. One of the largest river systems of the world with a major source of freshwater and sustains the livelihoods of 650 million people in its local and surrounding areas, this review study has great implications in terms of socioeconomic aspects as well. Therefore, this review study aims to analyze the variations of hydrochemistry with its controlling factors and assess the irrigation water quality.

2 Materials and Methods

2.1 Study area

River hydrochemistry and water quality for the irrigation purposes of tributaries in the GBRS, which are prominent for different domestic and development purposes, have been assessed in this review study based on hydrochemical information from the various published literature (Rai et al. 2010; Avtar et al. 2011; Khan et al. 2016; Banerjee and Ghosh 2016; Gupta et al. 2016; Paudyal et al. 2016; Das et al. 2016; Pant et al. 2018; Tsering et al. 2019; Liu et al. 2019). Major 12 tributaries of the GBRS (Yarlung-Tsangpo, Teesta, Brahmaputra, Rangit, Indrawoti, Dudhkoshi, Gandaki, Garra, Ken, Betwa, Gomti, and Damodar) were considered in this study.

The GBRS is a large Himalayan foreland basin formed after the collision of Eurasian and Indian plates that occurred 40-65 million years ago (Ding et al. 2016). The basin was further developed by the loading thrust and the regional lithospheric flexure (isostasy) during the period of Late Eocene to Miocene and upliftment of the northern part and subsidence of the southern part from mid-Miocene to the present day. The Ganga-Brahmaputra basin comprises Himalayan orogen lithostratigraphy (consisting of the Tethys Himalaya, Higher Himalaya, Lesser Himalaya, Siwalik domain, and the Indo-Gangetic Plain). The southern unit can be observed only in the Ganga basin and is absent in the Brahmaputra basin. Since its formation, the basin has received an uninterrupted supply of sediments from both the rising Himalaya and the Peninsular Cratonic sources, the production and delivery of which was primarily controlled by both climate and regional tectonics. The precipitation pattern in the GBRS is distinct from north to south. The Himalaya region of the GBRS has received comparatively higher precipitation. The southern region is also received higher precipitation but not as much as the Himalaya region. The upstream region especially the leeward side of the Himalaya has received comparatively lower precipitation (Fig. 1b). The land use/cover pattern of the GBRS is varied from Himalaya to the peninsular plain area. There exist about 29 land use/cover types with dominancy of forest land, agriculture/cultivated land, shrubland, built-up area, water bodies, grassland, etc. (Thenkabail et al. 2005) (Fig. 1c).

2.2 Data collection

The hydrochemical properties of the river stream are varied on the geology of the source and somehow contribution from the anthropogenic driver. For a better spatial comparison, only the pre-monsoonal ionic information of river hydrochemistry in the published literature had been collected and discussed. The following physicochemical parameters were taken for analyses: pH, total dissolved solids (TDS), electrical conductivity (EC), calcium (Ca^{2+}), magnesium (Mg^{2+}), sodium (Na^{+}), potassium (K^{+}), sulfate (SO_4^{2-}), chloride (Cl^-), bicarbonate (HCO_3^-), and nitrate (NO_3^-). There was a lacking EC value in some of the river hydrochemical datasets. The relation of TDS and EC for freshwater {$TDS=k \times EC$, k=constant factor (Walton 1989); and k =0.55 for freshwater (Rusydi 2018)} had been adopted to calculate the missing value of EC.

Except for Teesta (Tsering et al. 2019), Gandaki (Pant et al. 2018), and Yarlung Rivers (Liu et al. 2019), most of the literature only published an average value of different chemical concentrations in separate study areas without detailed information on hydrochemical attributes at the individual sampling location. Therefore, further chemical characterization and irrigation suitability analyses have been carried out for Teesta, Gandaki, and Yarlung Rivers for a deeper understanding of the spatial variation.

2.3 Chemical analyses

The Piper diagram, Gibbs plot, mixing diagram, and ionic ratios were used for the comprehensive elaboration of hydrochemistry. The Piper diagram is a trilinear shape diagram and one of the commonly used effective graphical procedures for presenting water chemistry data to help in understanding the nature and variations of the dissolved ions in water (Piper 1944). Generally, six sub-fields of chemical types can be identified in the diamond section of the Piper diagram: 1) Ca-HCO_3, 2) Na-Cl, 3) Mixed Ca-Na-HCO_3, 4) Mixed Ca-Mg-Cl, 5) Ca-Cl, and 6) Na-HCO_3 (Khadka and Ramanathan 2013; Pant et al. 2021). The Gibbs plot is also an analytical method to determine key factors of controlling the hydrochemistry of surface water. From the relation of the TDS versus $Na^+/(Na^++Ca^{2+})$ and the TDS versus $Cl^-/(Cl^-+HCO_3^-)$, three of the key processes including atmospheric precipitation, rock dominance, and evaporation-crystallization processes controlling surface water chemistry can be presented by the Gibbs plot (Gibbs 1970). The main application of the mixing diagram in hydrochemistry and ionic ratios is aimed to understand the types of minerals in the river catchment mainly including carbonates, silicates, and evaporates. The ionic ratios are also another analytical technique in hydrochemistry to support the results of the Piper diagram, Gibbs plot, and Mixing diagram.

2.4 Irrigation suitability assessment

The chemical and physical characteristics of river water using for irrigation purposes are the basic consideration for the irrigation water quality evaluation. Specific properties of irrigation water have relevant relation to the quantity and quality of crops, maintenance of soil properties, and surrounding environmental balance (Alobaidy et al. 2010; Bishwakarma et al. 2019). The Food Agriculture Organization (FAO) has provided the permissible limit for irrigation water standards according to the physicochemical parameters of irrigation water (Table 1). All the examined variables have been analyzed and compared with FAO guidelines and certain physicochemical parameters are taken for the scientific analysis of irrigation water quality, such as EC, Ca^{2+}, Mg^{2+}, Na^{+}, and K^{+} in this study based on the calculation of EC, sodium percentage (Na%), sodium percentage ratio (SAR), magnesium hazard (MH) and Wilcox diagram.

There exist different methods for the evaluation of irrigation water quality. The irrigation water quality had been studied individually with the following methods from the perspectives of salinity hazard, sodium hazard, magnesium hazard and comprehensive consideration:

i. EC: It is used for an indication of the salinity hazard which is the most significant water quality guideline on crop production (Salifu et al. 2017). The irrigation water quality referring to EC values is defined as follows (Ayers and Westcot 1985):

$$\mathrm{EC}\begin{cases} <700, & \text{Excellent} \\ [700, 3000], & \text{Good} \\ >3000, & \text{Fair} \end{cases} \quad \ldots\ldots\ldots\ldots (1)$$

ii. Na%: It is one of the widely used parameters indicating sodium content in irrigation water for the suitability assessment. Doneen (1954) proposed the following relation to calculate Na%.

$$\mathrm{Na\%} = \frac{\mathrm{Na^+ + K^+}}{\mathrm{Ca^{2+} + Mg^{2+} + Na^+ + K^+}} \times 100 \ldots\ldots\ldots (2)$$

$$\mathrm{Na\%}\begin{cases} <20, & \text{Excellent} \\ (20, 40), & \text{Good} \\ (40, 60), & \text{Permissible} \\ (60, 80), & \text{Doubtful} \\ >80, & \text{Unsuitable} \end{cases} \quad \ldots\ldots\ldots\ldots (3)$$

iii. SAR: It is a useful indicator of the level to which water undergoes cation exchange reactions in the soil (Joshi et al. 2009). The SAR is proposed by (Richards 1954) and calculated as:

$$\mathrm{SAR} = \frac{\mathrm{Na^+}}{\sqrt{(\mathrm{Ca^{2+} + Mg^{2+}})/2}} \ldots\ldots\ldots (4)$$

$$\mathrm{SAR}\begin{cases} <10, & \text{Excellent} \\ (10, 18), & \text{Good} \\ (18, 26), & \text{Fair} \\ >26, & \text{Poor} \end{cases} \quad \ldots\ldots\ldots\ldots (5)$$

iv. MH: It is a method for irrigation water quality assessment. The status of magnesium and calcium should be both in equilibrium for suitable irrigation purposes. Raghunath (1987) proposed the relation to calculate MH as follows:

$$\mathrm{MH} = \frac{\mathrm{Mg^{2+}}}{\mathrm{Ca^{2+} + Mg^{2+}}} \times 100 \ldots\ldots\ldots (6)$$

$$\mathrm{MH}\begin{cases} <50, & \text{Suitable} \\ \geq 50, & \text{Unsuitable} \end{cases} \quad \ldots\ldots\ldots\ldots (7)$$

v. Wilcox Diagram: The Wilcox diagram is also known as US Salinity diagrams proposed by Wilcox in 1948 and further improved from Torn in 1951. Nowadays, this diagram is commonly used for a comprehensive evaluation of irrigation water quality (Alavi et al. 2016). In the Wilcox diagram, irrigation water quality has been divided into C1, C2, C3 and C4 zones, based on the salinity hazard (EC) in the horizontal axis and S1, S2, S3, and S4 zones based on sodium hazard (SAR) in the vertical axis (Lokhande and Mujawar 2016). Water classification for agricultural uses according to the Wilcox classification is as Table 2.

3 Results and Discussion

3.1 Similarities and differences of the rivers

According to their similarities and differences in hydrochemical attributes, the average elevation of the river catchment, average annual river discharge, and annual precipitation in the studied rivers (Table 3) were categorized into two groups by performing hierarchical cluster analysis with Ward's method and Squared Euclidean distance which was also verified by principal component analysis. The resulting dendrogram and component plot are presented in Fig. 2. The rivers from the peninsular region were mostly categorized in Group-1 (Ken, Betwa, Gomti, Garra, and Damodar Rivers) and the rest of the rivers mainly

Table 2 Wilcox diagram classification (Alavi et al. 2016)

Section	Water quality for agriculture
C1S1	Sweet-completely effective for agriculture
C1S2, C2S2, C2S1	Brackish-approximate perfect for agriculture
C1S3, C2S3, C3S1, C3S2, C3S3	Passion-usable for agriculture
C4S4, C4S1, C1S4, C2S4, C3S4, C4S4, C4S3	Very passion-harmful to agriculture

Notes: All ionic concentrations are expressed in milli-equivalents per liter (meq/L) for the calculation of the above-mentioned irrigation parameters.

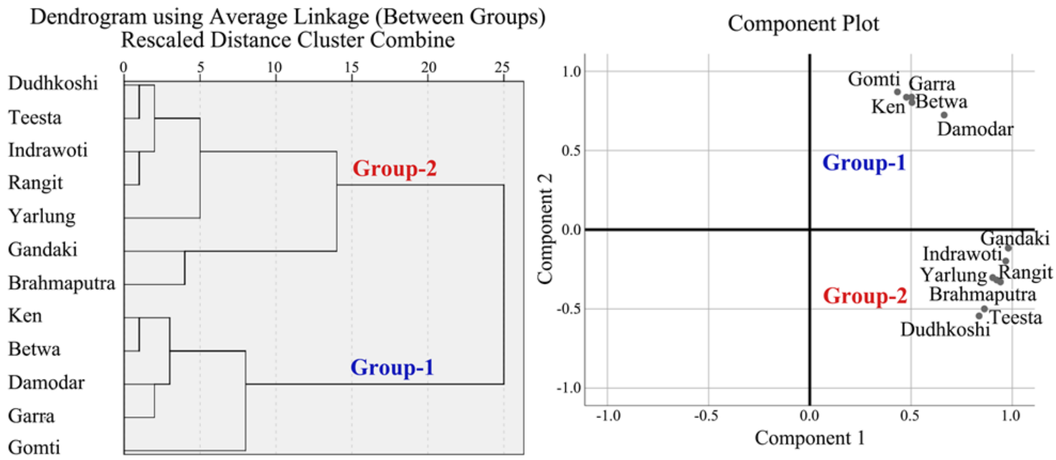

Fig. 2 Classification of rivers based on cluster analysis and principal component analysis.

Table 3 Average basin elevation, annual precipitation and discharge of the studied rivers

River Name	Average elevation (m)	Annual prec. (mm)	Annual discharge (m^3/s)
Ken	323	975	310
Betwa	341	975	658
Gomti	185	1025	234
Damodar	610	1100	296
Garra	160	875	NA
Gandaki	4094	2667	1753
Dudhkoshi	3073	1250	180
Indrawoti	1929	1250	75
Yarlung	3650	750	7700
Brahmaputra	5000	2300	21261
Teesta	3000	1150	532
Rangit	2500	1150	100

Notes: NA means not available; Prec. means precipitation.

originating from the Himalaya region (Yarlung-Tsangpo, Teesta, Brahmaputra, Rangit, Indrawoti, Dudhkoshi, and Gandaki) were categorized in Group-2 (Fig. 1a). Group-1 rivers are mostly draining through a southern region having comparatively moderate precipitation (average annual rainfall: 1000 mm). In addition, the average elevation of a river catchment in the Group-1 rivers is 325 m asl. The Group-2 rivers are mostly draining through the Himalaya region having relatively higher precipitation except for the Yarlung River (average annual rainfall: 1500mm; Yarlung: 750 mm). In addition, the average elevation of a river catchment in the Group-2 Rivers is 3300 m asl. Furthermore, we have done principal component analysis (PCA) for the validation of the cluster analysis. The PCA analysis with varimax rotation explaining 95.75% of the total variance also showed the same classification of the studied river as cluster analysis (Appendix 1).

3.2 General hydrochemistry

The concentrations of dissolved solutes were compared to find out the ionic distribution patterns in rivers among the two groups of rivers in the GBRS (Table 4). The pH of all the rivers in Group-1 and Group-2 was found slightly alkaline to alkaline nature with an average value of 8.01±0.19 and 8.02±0.55, respectively. As compared with individuals, the pH value is slightly higher in the Gandaki, and Yarlung Rivers mainly draining from the Himalaya region. The average values of EC in Group-1 and Group-2 were found to be 378±185 µS/cm and 214±140 µS/cm, respectively. The average value of EC was significantly higher in Group-1. The average value of TDS was

Table 4 Concentrations of major ions in the Ganges-Brahmaputra River System (GBRS); Ionic values are expressed in (μeq/L), TDS in (mg/L) and EC in (μS/cm)

	River Name	pH	EC	TDS	Ca^{2+}	Mg^{2+}	Na^{+}	K^{+}	SO_4^{2-}	Cl^{-}	NO_3^{-}	HCO_3^{-}	Study Period	Accuracy of determination
Group 1	Ken[a]	8.20	327	284	1252	1041	725	88	1383	477	5	2342	April 2007	NA
	Betwa[a]	7.90	279	237	1529	770	536	61	1425	490	6	2453	April 2007	NA
	Gomti[b]	8.25	705	388	1744	1788	1354	127	504	400	17	4193	NA	NICB: <3%
	Garra[c]	7.85	252	136	1542	974	888	68	221	106	25	2822	March 2014	NA
	Damodar[d]	7.87	326	211	1028	918	801	154	424	366	12	2099	Premonsoon 2016	NA
	Average	8.01	378	251	1419	1098	861	100	791	368	13	2782		
Group 2	Gandaki[e]	8.50	675	340	2520	1461	843	97	1478	790	14	2530	April 2016	R^2: 0.99
	Dudhkoshi[f]	7.52	69	38	395	33	35	18	77	17	19	361	May 2013	R^2: 0.74
	Indrawoti[f]	8.18	176	97	750	283	183	28	188	56	65	951	May 2013	R^2: 0.94
	Yarlung[g]	8.67	334	184	1336	502	417	39	625	210	13	1309	May 2016	R^2: 0.98
	Brahmaputra[h]	7.42	171	118	1091	524	319	60	395	132	19	1858	April 2013	NA
	Teesta[i]	7.69	120	66	473	116	137	33	213	25	-	527	March 2018	NA
	Rangit[j]	7.49	73	64	429	301	192	468	348	241	14	1130	March 2014	NA
	Average	7.91	200	114	906	394	225	102	356	121	24	1210		
Global average[k]		8.00	-	120	750	342	274	59	233	220	16	957		

a: (Avtar et al. 2011); b: (Rai et al. 2010); c: (Khan et al. 2016); d: (Banerjee and Ghosh 2016); e: (Pant et al. 2018); f: (Paudyal et al. 2016); g: (Liu et al. 2019); h: (Das et al. 2016); i: (Tsering et al. 2019); j: (Gupta et al. 2016); k: (Gaillardet et al. 1999); NA: Not available; R^2: Regression coefficient; NICB: Normalized inorganic charge balance.

found 251±93 mg/L and 121±68 mg/L in Group-1 and Group-2, respectively. As compared individually, the average values of EC and TDS in Gomti (Group-1), and Gandaki (Group-2) had been observed higher than the others. Different factors were affecting the EC and TDS in river water. The intense interaction of bed-rock with flowing water possibly increased the EC and TDS values (Ansari and Ahmad, 2019). Also, the high relief, tectonic disturbance, and large-scale anthropogenic stresses were responsible to increase TDS and EC of river water (Chakrapani 2005). The TDS values in most of the tributaries in the GBRS were greater than the global average (120 mg/L) except for some Himalaya rivers, such as Teesta, Brahmaputra, Rangit, Dudhkoshi, and Indrawoti. The lower TDS was possibly due to very few human disturbances, originating from a glacier-fed and flowing from high elevation stretches with less bed-rock interaction.

The ionic concentrations of rivers in the GBRS were categorized into two groups as described above. Generally, HCO_3^-, SO_4^{2-}, Ca^{2+}, Mg^{2+}, and Na^+ were dominant ions among the observed dissolved materials in river water (Meybeck 1987). The average concentration of major ions together with pH and TDS had been plotted in Box plot to identify the significant difference among the two groups (Fig. 3). The average concentrations of major dissolved solutes were found significantly different. The average concentrations of most of the physicochemical parameters showed significantly higher in Group-1, i.e., TDS, EC, Ca^{2+}, Mg^{2+}, Na^+, Cl^- and HCO_3^-. The average concentrations of NO_3^- had been found highest in Group-2 especially in the Indrawoti River (65 μeq/L). The higher concentration of NO_3^- in the Indrawoti River was associated with anthropic activities such as excessive use of N-containing chemical fertilizers in the vicinity of the river channel (Paudyal et al. 2016). The comparative abundance of major cations and anions among the two groups in the GBRS had been attempted. The same as global average order, the anionic and cationic abundancy based on the average values (μeq/L) of the two groups were in the following order: $HCO_3^- > SO_4^{2-} > Cl^- > NO_3^-$ and $Ca^{2+} > Mg^{2+} > Na^+ > K^+$, respectively. HCO_3^- was most dominant and NO_3^- was the least dominant anion over the GBRS. Whereas, Ca^{2+} and K^+ were the most and least dominant cations, respectively. The relatively higher concentrations of HCO_3^- and Ca^{2+} indicated the contribution of rock weathering as the main processes that determined the hydrochemistry of river catchment (Pant et al. 2018).

The spatial variations of general hydrochemistry of the three rivers from Group-2 as shown in Table 5 and had been analysed separately for a deeper understanding. In both upstream and downstream,

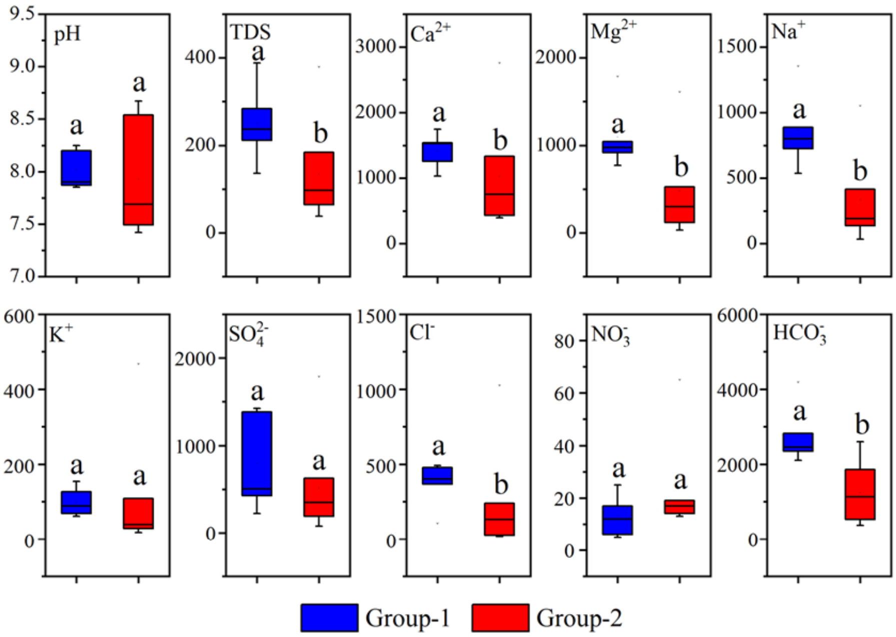

Fig. 3 Box plots of major ions, showing a comparison among Group-1 and Group-2 in the GBRS (Ionic values are expressed in μeq/L, except TDS in mg/L). The alphabet associated with the ionic values represent the significant difference (p<0.05).

Table 5 Concentrations of major ions in the Teesta, Yarlung and Gandaki Rivers; Ionic values are expressed in (μeq/L), TDS in (mg/L) and EC in (μS/cm)

River Name	pH	EC	TDS	Ca^{2+}	Mg^{2+}	Na^+	K^+	SO_4^{2-}	Cl^-	NO_3^-	HCO_3^-
Teesta-Upstream	7.48	111	61	529	90	112	24	254	13	4	473
Teesta-Downstream	7.88	129	71	482	144	165	43	196	36	4	614
Yarlung-Upstream	NA	422	232	2083	585	44	68	570	436	14	2054
Yarlung-Midstream	NA	404	222	1998	615	526	48	844	194	18	1862
Yarlung-Downstream	NA	298	164	1519	471	322	40	691	118	19	1509
Gandaki-Upstream	8.66	1045	524	3637	2215	1811	149	2923	1877	14	2871
Gandaki-Downstream	8.42	463	234	1873	1002	292	68	649	172	15	2338

the ionic dominancy of Teesta rivers followed: HCO_3^- >SO_4^{2-} >Cl^- >NO_3^- and Ca^{2+} >Na^+ >Mg^{2+} >K^+ for anions and cations, respectively. And major ions together with TDS, and EC, showed a non-significant difference between upstream and downstream. The variations in upstream, midstream, and downstream of Yarlung River suggested significant spatial variations of hydrochemistry. The ionic dominancy of Yarlung rivers followed: HCO_3^->SO_4^{2-}>Cl^->NO_3^- and Ca^{2+}>Mg^{2+}>Na^+>K^+ for anions and cations in all three segments. However, the concentration of major ions such as Ca^{2+}, K^+, Cl^- and HCO_3^- together with EC and TDS were higher in the upstream whereas the concentration of Mg^{2+}, Na^+, and SO_4^{2-} were higher in the midstream and the concentration of NO_3^- was slightly higher in the downstream region. The general hydrochemistry of the Gandaki River showed significant variations in upstream and downstream. The anionic dominancy of Gandaki River followed: SO_4^{2-}>HCO_3^->Cl^->NO_3^- and HCO_3^->SO_4^{2-}>Cl^->NO_3^- in upstream and downstream, respectively. Whereas, the cationic dominancy followed the same order of Ca^{2+}>Mg^{2+}>Na^+>K^+ in both upstream and downstream. All the physicochemical concentrations reported were higher in upstream than downstream except NO_3^-, which indicates the anthropogenic signatures in the downstream segments of the Gandaki River Basin.

3.3 Characterization of hydrochemistry

The ionic concentrations of rivers in the GBRS was plotted in the Piper diagram and further projected into the central diamond field to characterize the hydrochemistry of the GBRS. On the left ternary (cation section), the plots indicated the dominancy of Ca^{2+} and Mg^{2+} types i.e. the carbonate dominated lithology over river catchment. The Rangit

River showed a higher percentage of Na^{+}+K^{+} due to the weathering of phyllite and mica schist over the river catchment (Gupta et al. 2016). On the right ternary (anion section), all the plots were in the location of the left corner showing the dominance of bicarbonate type (HCO_3^-) which also indicated carbonate lithology. The diamond field of the Piper diagram revealed the overall characteristics of the GBRS: the dominancy of the alkaline earth elements (Ca^{2+} and Mg^{2+}) over the alkaline (Na^{+} and K^{+}) and the weak acids (HCO_3^-) over the strong acids (Cl^- and SO_4^{2-}) (Fig. 4).

The hydrochemical facies of Teesta, Yarlung, and Gandaki Rivers with spatial variations plotted in the piper diagram (Fig. 5) showed the dominancy of the Calcium-bicarbonate type of hydrochemistry except the upstream of Gandaki River. The upstream of the Gandaki River plotted into the middle of the diamond plot showed the mixed type of hydrochemistry. The reason for this mechanism in upstream of Gandaki was due to the influence of local sources of Na^{+} and K^{+} over river catchment (Pant et al. 2018). There was a significant variation of hydrochemistry among upstream, midstream, and downstream in Yarlung river stretches. However, all three segments were plotted into calcium bicarbonate types of hydrochemistry indicating the dominancy of Ca^{2+} and HCO_3^- over cationic and anionic budget. Similarly, the piper diagram revealed the calcium-bicarbonate type of hydrochemistry in both the upstream and downstream of the Teesta River stretch.

3.4 Major sources and controlling mechanism

The average hydrochemical attributes was explored in the Gibbs plot to find out the major natural controlling factors of the river hydrochemistry (Fig. 6). The ionic distributions were characterized by relatively moderate TDS and low ratios of $Na^{+}/(Na^{+}+Ca^{2+})$ or $Cl^{-}/(Cl^{-}+HCO_3^{-})$. Comparatively, the ratio of $Na^{+}/(Na^{+}+Ca^{2+})$ and $Cl^{-}/(Cl^{-}+HCO_3^{-})$ in the Group-1 rivers is higher than the Group-2. Illustrating the dominance of geogonic factors, the Gibbs plot showed rock weathering was the major natural controlling mechanism in the GBRS.

The Gibbs plot prepared for Teesta, Yarlung, and Gandaki Rivers (Fig. 7) also suggested that the natural rock weathering was the major controlling natural factor of hydrochemistry over the river basin. However, the ratio of $Na^{+}/(Na^{+}+Ca^{2+})$ or $Cl^{-}/(Cl^{-}+HCO_3^{-})$ in the upstream of the Gandaki River was relatively higher than the downstream also had a higher TDS. This was evidence of the minor role of evaporation-crystallization processes for controlling the hydrochemistry in the upstream region. But the downstream of the Gandaki River showed the control of the rock weathering. The low ratio of $Na^{+}/(Na^{+}+Ca^{2+})$ or $Cl^{-}/(Cl^{-}+HCO_3^{-})$ and moderate TDS of the Teesta and Yarlung rivers indicating natural rock weathering plays a vital role to control the hydrochemistry. There were no significant differences in upstream and downstream of Teesta River and upstream, midstream, downstream of

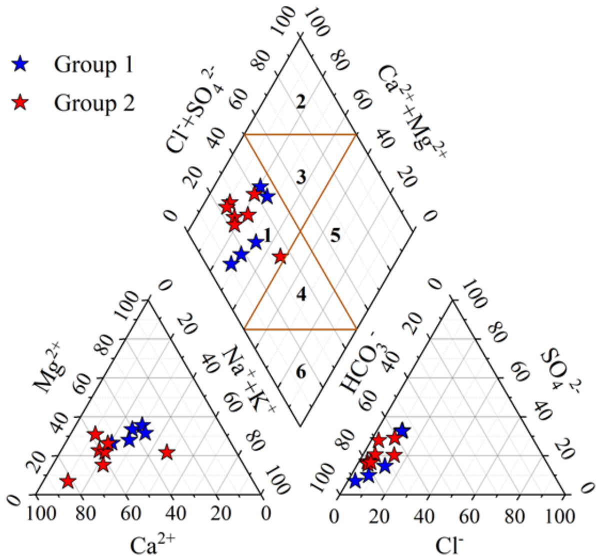

Fig. 4 Piper diagram characterizing the hydrochemical facies among Group-1 and Group-2, Rivers of the GBRS.

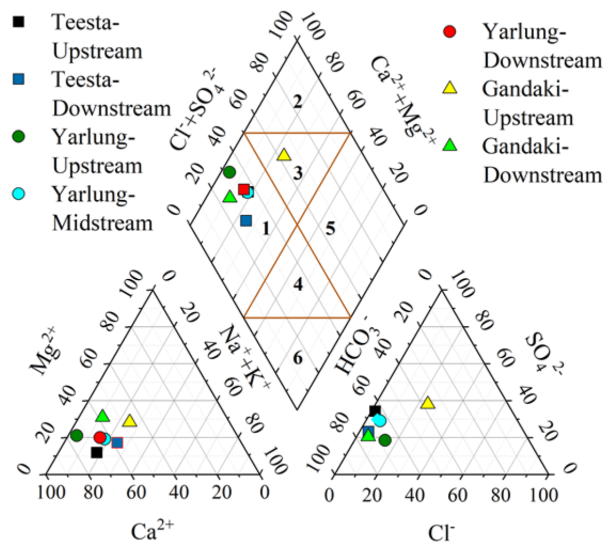

Fig. 5 Piper diagram showing the hydrochemical facies of Teesta, Yarlung, and Gandaki Rivers.

Yarlung River, despite the geological variations.

The Na^+-normalized Ca^{2+} vs. Mg^{2+} and Na^+ -normalized Ca^{2+} vs. HCO_3^- ratios were plotted to evaluate the presence of carbonates, silicates, and evaporites minerals over the river basin (Gaillardet et al. 1999). The average values of hydrochemical attributes of different rivers of the Group-1 and Group-2 of the GBRS had been plotted into the mixing diagram (Fig. 8). The plots of all the rivers located between the carbonates and silicates end members indicating the dominancy of carbonate and silicate minerals in the GBRS. The mixing diagram further illustrated that the rivers in Group-1 Rivers moved to silicates domain and Group-2 Rivers moved to carbonates domain exhibited the lowland and highland region of the GBRS was mainly dominated by silicate carbonate minerals, respectively.

Another mixing diagram had been plotted for Teesta, Yarlung, and Gandaki Rivers using average ionic ratio in spatial scale (Fig. 9). The upstream of Gandaki River plotted towards silicate end member and upstream of the Yarlung River plotted towards the carbonates end member indicated the hydrochemistry of upstream of the Gandaki and upstream of the Yarlung were driven by the silicate rock weathering and carbonate rock weathering, respectively. The rest were plotted between the silicates and carbonate end members suggesting carbonate and silicate rock weathering were the keys responsible to control the hydrochemistry.

The relationships among ions and ionic ratios are used to evaluate the sources of dissolved ions and controlling mechanisms of hydrochemistry in the freshwater system (Yde et al. 2008; Feng et al. 2012; Ansari and Ahmad 2019). The ionic ratios of the two groups were presented in Table 6. The ratio of HCO_3^- /Ca^{2+} was <2 suggesting the control of carbonate rock weathering in the GBRS (Thomas et al. 2015). Moreover, the high mean ratios of $(Ca^{2+}+Mg^{2+})/(Na^++K^+)$ (2.62: Group-1 and 4.34: Group-2) and $HCO_3^-/(Na^++K^+)$ (2.90: Group-1 and 3.97: Group-2) supported to proven the dominancy of weathering of dolomite and calcite minerals. The high ratios of $(Ca^{2+}+Mg^{2+})/Tz^+$ (0.72: Group-1 and 0.81: Group-2) also suggested the domination of carbonate weathering and the comparatively low ratios of $(Na^++K^+)/Tz^+$ indicated less intense evaporates over carbonate weathering in the GBRS. The HCO_3^- /$(HCO_3^-+SO_4^{2-})$ (C-ratio) explained the relative importance of carbonation and sulfide oxidation. If the C-ratio is <0.50, the coupled chemical reactions of both carbonate dissolution and sulfide oxidation are indicated, whereas if the ratio is close to 1, exclusively carbonation reactions and dissociation of CO_2

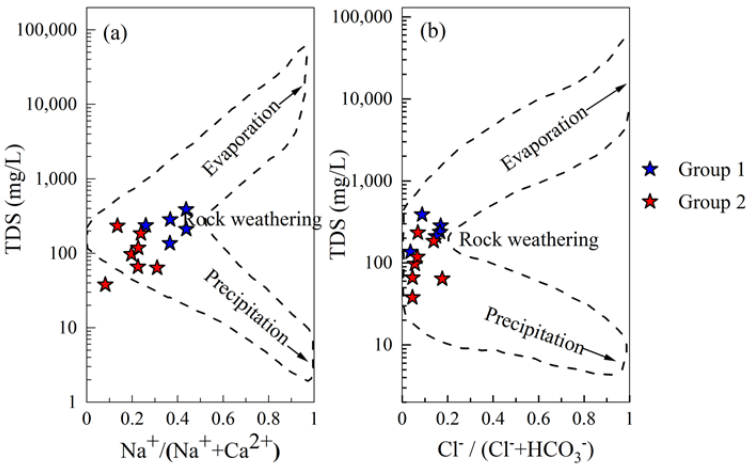

Fig. 6 Gibbs plot of the Group-1 and Group-2 Rivers of the GBRS.

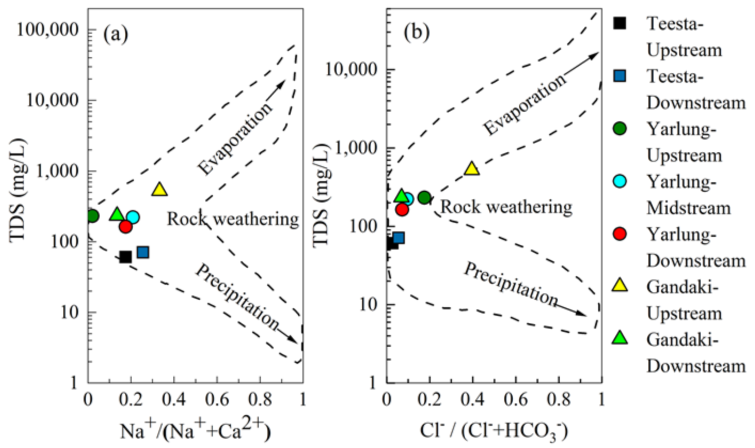

Fig. 7 Gibbs plot of the Teesta, Yarlung, and Gandaki Rivers.

Table 6 Ionic ratios among hydrochemical attributes (all the ionic ratios were derived from μeq/L)

Ionic Ratio	Group-1	Group-2
HCO_3^- / Ca^{2+}	1.96	1.34
HCO_3^- / (Na^++K^+)	2.90	3.70
$(Ca^{2+}+ Mg^{2+})$ / $(Na^++ K^+)$	2.62	3.98
HCO_3^- / $(HCO_3^-+ SO_4^{2-})$	0.78	0.77
$(Ca^{2+}+ Mg^{2+})$ / TZ^+	0.72	0.80

deriving protons from atmospheric inputs. The C-ratios (0.78: Group-1 and 0.77: Group-2) specified the major role of carbonate and CO_2 dissolution in proton producing mechanism in the GBRS.

3.5 Suitability for irrigation quality

Irrigation suitability of the major 12 tributaries in the GBRS was evaluated using different methods and presented in Table 7 and Fig. 10. The average ionic concentrations of River water including pH and TDS were compared with the permissible limits of FAO guidelines for irrigation water and suggested that all the Rivers were within the permissible limits. The EC values were ranges 69-754 μS/cm in the GBRS and suggested all the rivers were in the "good and excellent" categories and concluded that all the rivers were acceptable for irrigation usage. The Na% in tributaries of the GBRS ranging 10.96-47.49, and were categorized in "Excellent to permissible". This also suggested all the rivers were acceptable to use for irrigation purposes from the perspective of Na%. However, the Rangit River has higher sodium content exhibiting the permissible for the irrigation analysis. The long-term utilization of Rangit River water for irrigation might be resulted in the formation of alkali soils due to the higher Na% combining with carbonate. Similarly, SAR values of all the rivers were less than 10 (ranges 0.08-1.02) and indicated the "Excellent" category which suggested all the river's water could be used for irrigation. The high magnesium content in water would cause more alkaline which would further affect crop yields and decrease the soil permeability. So, MH content (magnesium hazard) in irrigation water less than 50 is acceptable for irrigation purposes. Based on the limited MH value, most of the tributaries in the GBRS were suitable except for the Gomti River. The concentration of Mg^{2+} in the Gomti River (50.62) was high due to anthropogenic contributions. Discharge of wastewater to the Gomti River channel increased by 10%-20% of the Mg^{2+} content in river water (Rai et al. 2010). The higher Mg^{2+} content in the Gomti River might alter the salinity of river water, increase the pH of the soil, affect the permeability properties of the soil root zone.

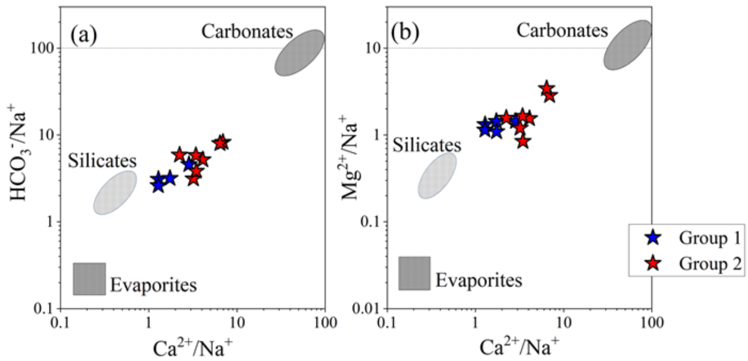

Fig. 8 Mixing diagram of Na-normalized molar ratios of (a) Ca^{2+} vs. HCO_3^- and (b) Ca^{2+} vs. Mg^{2+} of the Group-1 and Group-2 Rivers.

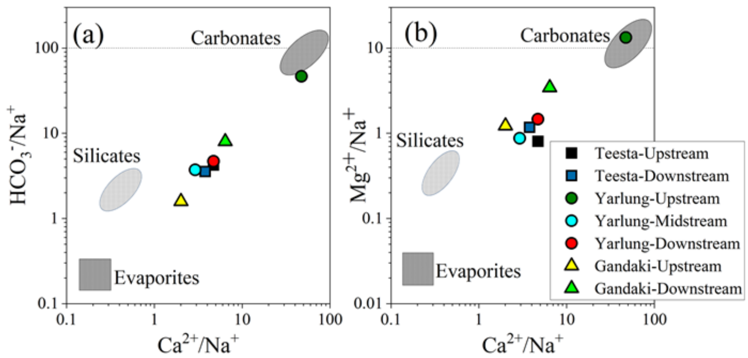

Fig. 9 Mixing diagram of Na-normalized molar ratios of (a) Ca^{2+} vs. HCO_3^- and (b) Ca^{2+} vs. Mg^{2+} of the Teesta, Yarlung, and Gandaki Rivers.

The irrigation water quality of Teesta, Yarlung and Gandaki Rivers with their spatial scale also suggested that the river water could be used for irrigation without any treatment and their ionic concentrations were within the FAO permissible limits. The details of irrigation suitability were presented in Table 8. All the parameters that we had checked in this review study indicated that the river water from upstream, midstream, and downstream of Teesta, Yarlung and Gandaki Rivers were in a safe condition for irrigational utilization. The higher EC in upstream of the Gandaki River may cause the degradation of soil permeability.

After the interpretation of the Wilcox diagram (Fig. 11), indicating the two classes: C1S1 and C2S1. The results of the Dudhkoshi, Rangit, Teesta, Brahmaputra, and Indrawoti plotted in C1S1 (low salinity and low sodium hazard) category indicated the best quality for irrigation purposes which were completely effective for agriculture. Likewise, Gharra,

Table 7 Irrigation suitability evaluation table of the major 12 tributaries of the Ganges-Brahmaputra River System (GBRS)

Rivers	EC	Class	Na%	Class	SAR	Class	MH	Class
Ken River	327	E	26.15	G	0.68	E	45.41	S
Betwa River	279	E	20.62	G	0.50	E	33.50	S
Gomti River	705	G	29.54	G	1.02	E	50.62	U
Damodar River	326	E	32.93	G	0.81	E	47.16	S
Garra River	252	E	27.52	G	0.79	E	38.72	S
Gandaki River	754	G	18.11	E	0.65	E	36.35	S
Dudhkoshi River	69	E	10.96	E	0.08	E	7.78	S
Indrawoti River	176	E	16.94	E	0.25	E	27.42	S
Yarlung River	334	E	19.86	E	0.43	E	27.30	S
Brahmaputra River	171	E	18.97	E	0.35	E	32.45	S
Teesta River	120	E	22.48	G	0.25	E	19.67	S
Rangit River	73	E	47.49	P	0.32	E	41.22	S
Average	310	E	21.37	E	0.43	E	32.82	S

Notes: E: Excellent, G: Good, P: Permissible, S: Safe/Suitable, U: Unsafe/Unsuitable.

EC means electrical conductivity (μS/cm), Na% means sodium percentage, SAR means sodium adsorption ratio, MH means magnesium hazard (Dimensionless).

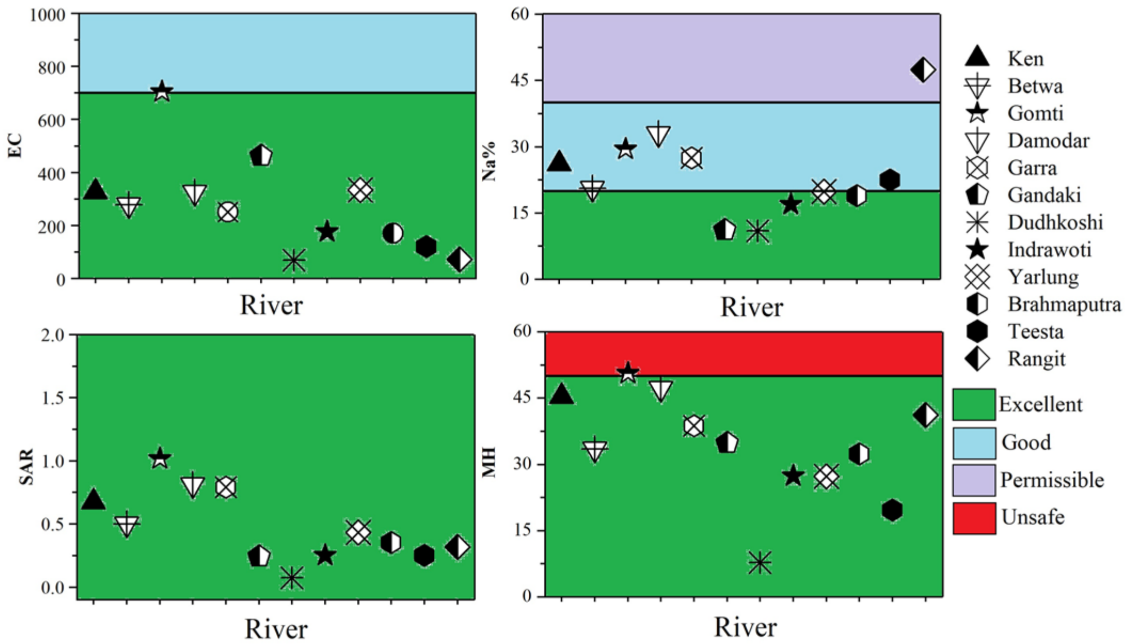

Fig. 10 Graphical representation of irrigation water quality of the GBRS.

Betwa, Yarlung, Damodar, Ken, Gandaki and Gomti River plotted in C2S1 (medium salinity and low sodium hazard) category suggested approximately perfect for agriculture. Overall interpretation of the Wilcox diagram also suggested the safe condition of river water in the GBRS for irrigational utilization.

4 Conclusion

This review study analyzed and expressed the hydrochemical characterization and irrigation suitability of 12 small and medium tributaries in the GBRS during the pre-monsoon season using available hydrochemical attributes collected from published literature. The hydrochemistry of the GBRS indicated a slightly alkaline to alkaline nature. The average concentrations of most of the chemical variables showed significantly higher in Group-1 except SO_4^{2-}, K^+ and NO_3^-. The grand mean values of the major anions and cations values in all rivers follow the order of $HCO_3^- > SO_4^{2-} > Cl^- > NO_3^-$ and $Ca^{2+} > Mg^{2+} > Na^+ > K^+$, respectively, the same as the global average order. Piper diagram implied that the river water hydrochemistry belongs to the Calcium-bicarbonate (Ca-HCO_3) type. The river water hydrochemistry was

Table 8 Irrigation suitability evaluation table of Teesta, Yarlung, and Gandaki Rivers

ID	EC	Class	Na%	Class	SAR	Class	MH	Class
Teesta-Upstream	111	E	18.01	E	0.20	E	14.54	S
Teesta-Downstream	129	E	24.94	G	0.29	E	23.00	S
Yarlung-Upstream	422	E	4.03	E	0.04	E	21.93	S
Yarlung-Midstream	404	E	18.01	E	0.46	E	23.54	S
Yarlung-Downstream	298	E	15.39	E	0.32	E	23.67	S
Gandaki-Upstream	1045	G	25.09	G	1.06	E	37.85	S
Gandaki-Downstream	463	E	11.13	E	0.24	E	34.85	S

Notes: All values were were expressed in meq/L. E: Excellent, G: Good, P: Permissible, S: Safe/Suitable, U: Unsafe/Unsuitable

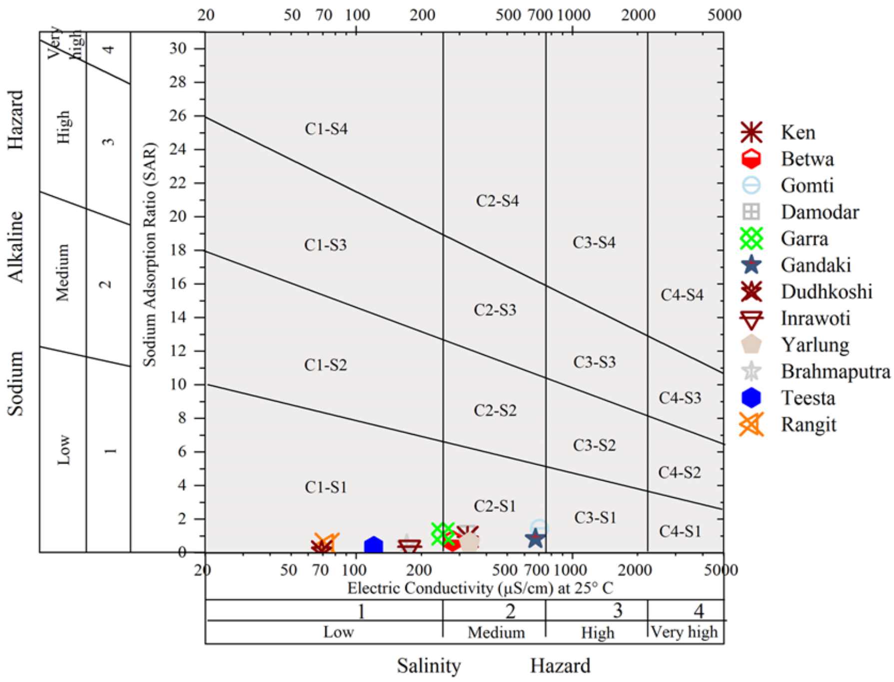

Fig. 11 Wilcox diagram for classifying irrigation suitability of the river water.

dominated by the carbonate and silicate rock weathering which was confirmed by the Gibbs plot and mixing diagram. Furthermore, the low ionic ratio of $(Na^{+}+K^{+})/TZ^{+}$, high ratio of $(Ca^{2+}+Mg^{2+})/TZ^{+}$, and the high C-Ratio, suggesting carbonate weathering was the dominance process. The river hydrochemistry of Teesta, Yarlung and Gandaki Rivers also indicated a slightly alkaline to alkaline nature with the dominancy of calcium-bicarbonate types except in upstream of the Gandaki River. Owing to the different geological and edaphic characters, the upstream of the Gandaki River plotted into the middle of the diamond plot showing mixed types of hydrochemistry. Gibbs diagram of upstream, midstream, and downstream of Teesta, Yarlung, and Gandaki Rivers indicated that natural rock weathering was a major natural controlling mechanism of river hydrochemistry. The carbonate and silicate rock weathering predominantly controlled the hydrochemistry of these rivers. The upstream of the Gandaki River and upstream of Yarlung River were controlled by silicate rock weathering and carbonate rock weathering, respectively. As a conclusion of hydrochemical characterization of the some selected small and medium tributaries of the GBRS, it clearly showed that the majority of the hydrochemical facies were Ca-HCO_3 type with the dominancy of the natural carbonate rock weathering followed by silicate rock weathering as a controlling mechanism. The contribution of evapo-crystallization in the hydrochemical budget of the GBRS was very minimal.

The suitability of river water for irrigation purposes was assessed during the pre-monsoon season by adopting different parameters, methods, and internationally accepted standards. All the rivers included in this review study were within the FAO limit and indicated being appropriate for irrigation using purpose based on EC, SAR, and Na%. However, The Gomti River is in the unsafe category according to MH. Long-term use of irrigation water with relatively higher content of Na^+ and Mg^{2+} in Rangit River and Gomti River might have resulted in the increasing pH of the soil, affect the permeability properties of the soil root zone and reduce the availability of phosphorous nutrients. Wilcox diagram revealed that all rivers could be used for irrigation purposes with plots on the major two sections (C1S1 and C2S1). In addition, the irrigation suitability assessment of Teesta, Yarlung, and Gandaki Rivers also showed the suitability for irrigation use. In conclusion, the river water in the GBRS was suitable for irrigation except for a few instances which need special caution for utilization. However, the responds of the hydrochemical characteristics and water quality to climate change are not clear in this region for lacking different periods studies which need persistent efforts by global scientists and local governments.

Acknowledgments

This study was financially supported by National Natural Science Foundation of China (Grant No. 41761144078) and Kathmandu Center for Research and Education, CAS-TU, Kathmandu, 44618, Nepal. The authors are obliged to Dr. Ramesh Raj Pant from Tribhuvan University, Nepal for his valuable comments and suggestions to this review work. Also, we would like to thank all the original research work used in this review paper. Finally, the authors would like to thank the anonymous reviewers for their constructive comments and suggestions which greatly help to polish the manuscript.

Electronic supplementary material: Supplementary material (Appendix 1) is available in the online version of this article at https://doi.org/10.1007/s11629-021-6834-z

References

Acharya A, Sharma, ML, Bishwakarma K, et al. (2020) Chemical characteristics of the Karmanasha river water and its appropriateness for irrigational usage. J Nepal Chem Soc 41: 94-102. https://doi.org/10.3126/jncs.v41i1.30494

Al-Shammiri M, Al-Saffar A, Bohamad S, et al. (2005) Waste water quality and reuse in irrigation in Kuwait using microfiltration technology in treatment. Desalination 185(1-3): 213-225. https://doi.org/10.1016/j.desal.2005.02.078

Alavi N, Zaree E, Hassani M, et al. (2016) Water quality assessment and zoning analysis of Dez eastern aquifer by Schuler and Wilcox diagrams and GIS. Desalin. Water Treat 57(50): 23686-23697. https://doi.org/10.1080/19443994.2015.1137786

Alobaidy AH, Al-Sameraiy MA, Kadhem AJ, et al. (2010) Evaluation of treated municipal wastewater quality for irrigation. J Environ Prot Ecol 01(03): 216-225.https://doi.org/10.4236/jep.2010.13026

Ansari Z, Ahmad S (2019) Hydro-geochemical characteristics of the Himalayan streams. J Appl Geochem 21(2): 225-237.

Avtar R, Kumar P, Singh CK, et al. (2011) A comparative study on hydrogeochemistry of Ken and Betwa rivers of Bundelkhand using statistical approach. Water Qual., Expo. Health 2(3-4): 169-179. https://doi.org/10.1007/s12403-010-0035-2

Ayers RS, Westcot DW (1985) Water quality for agriculture. In FAO of the UNITED NATIONS, Rome, Italy.

Banerjee R, Ghosh AR (2016) Spatio-temporal analysis of water quality trends in the middle stretch of the river Damodar. Int J Sci Res Sci Technol 2(6): 191-198.

Bishwakarma K, Pant RR, Pal KB, et al. (2019) Water quality and land use/cover changes in the Phewa watershed, Gandaki Province, Nepal. Nepal J Environ Sci 7: 31-39. https://doi.org/10.3126/njes.v7i0.34473

Chakrapani GJ (2005) Major and trace element geochemistry in upper Ganga river in the Himalayas, India. Environ Geol 48(2): 189-201. https://doi.org/10.1007/s00254-005-1287-1

Das P, Sarma KP, Jha PK, et al. (2016) Understanding the cyclicity of chemical weathering and associated CO2 consumption in the Brahmaputra river basin (India): the role of major rivers in climate change mitigation perspective. Aquat Geochem 22(3): 225-251. https://doi.org/10.1007/s10498-016-9290-6

Dekov VM, Komy Z, Araújo F, et al. (1997) Chemical composition of sediments, suspended matter, river water and ground water of the Nile (Aswan-Sohag traverse). Sci Total Environ 201(3): 195-210. https://doi.org/10.1016/S0048-9697(97)84057-0

Ding L, Qasim M, Jadoon IAK, et al. (2016) The India-Asia collision in north Pakistan: insight from the U-Pb detrital zircon provenance of cenozoic foreland basin. Earth Planet Sci Lett 455(2001): 49-61. https://doi.org/10.1016/j.epsl.2016.09.003

Doneen L (1954) Salination of soil by salts in the irrigation water. Am Geophys Union 35: 3-7.

Feng F, Li Z, Jin S, et al. (2012) Hydrochemical characteristics and solute dynamics of meltwater runoff of Urumqi Glacier No.1, eastern Tianshan, northwest China. J Mt Sci 9(4): 472-482. https://doi.org/10.1007/s11629-012-2316-7

Fipps G (1995) Standards and salinity management and salinity management water analysis. Agril Exten 4(3): 1-17.

Gaillardet J, Dupre B, Louvat P, et al. (1999) Global silicate weathering and CO2 consumption rates deduced from the chemistry of large rivers. Chem Geol 159(1-4): 3-30. https://doi.org/10.1016/S0009-2541(99)00031-5

Gibbs RJ (1970) Mechanisms controlling world water chemistry. Science 170(3962): 1088-1090. https://doi.org/10.1126/science.170.3962.1088

Gupta S, Nayek S, Chakraborty D (2016) Hydrochemical evaluation of Rangit river, Sikkim, India: using water quality index and multivariate statistics. Environ Earth Sci 75(7). https://doi.org/10.1007/s12665-015-5223-8

Haidary A, Amiri BJ, Adamowski J, et al. (2013) Assessing the impacts of four land use types on the water quality of wetlands in Japan. Water Resour Manag 27(7): 2217-2229. https://doi.org/10.1007/s11269-013-0284-5

Huang X, Sillanpää M, Duo B, et al. (2008) Water quality in the Tibetan Plateau: metal contents of four selected rivers. Environ Pollut 156(2): 270-277. https://doi.org/10.1016/j.envpol.2008.02.014

Huang X, Sillanpää M, Gjessing ET, et al. (2009) Water quality in the Tibetan Plateau: major ions and trace elements in the headwaters of four major Asian rivers. Sci Total Environ 407(24): 6242-6254. https://doi.org/10.1016/j.scitotenv.2009.09.001

Jiang L, Yao Z, Liu Z, et al. (2015) Hydrochemistry and its controlling factors of rivers in the source region of the Yangtze river on the Tibetan Plateau. J Geochem Explor 155: 76-83. https://doi.org/10.1016/j.gexplo.2015.04.009

John DM, Rpbert HM (1983) World-wide delivery of river sediment

to the oceans. J Geol 91: 1-21.
Joshi DM, Kumar A, Agrawal N (2009) Assessment of the irrigation water quality of river Ganga in Haridwar district. Rasayan J Chem 2(2): 285-292.
Khadka UR, Ramanathan AL (2013) Major ion composition and seasonal variation in the Lesser Himalayan lake: case of Begnas Lake of the Pokhara Valley, Nepal. Arab J Geosci 6(11): 4191-4206. https://doi.org/10.1007/s12517-012-0677-4
Khan MYA., Khan B, Chakrapani GJ (2016) Assessment of spatial variations in water quality of Garra River at Shahjahanpur, Ganga Basin, India. Arab J Geosci 9(8). https://doi.org/10.1007/s12517-016-2551-2
Kuehl S, Allison AMA, Goodbred SL (2011) The Ganges-Brahmaputra Delta. River Deltas-Concepts, Models, and Examples. Spec. Publ. - SEPM 83: 413-434.https://dx.doi.org/10.2110/pec.05.83.0413
Kumari P (2017) Irrigation water quality based on hydro chemical analysis of Ganga-Sone Divide Region of Bihar. Asian J Water, Environ Pollut 14(3): 75-83.https://doi.org/10.3233/AJW-170028
Liu J, Zhao Y, Li Z, et al. (2019) Quantitative source apportionment of water solutes and CO2 consumption of the whole Yarlung Tsangpo River basin in Tibet, China. Environ Sci Pollut Res 26(27): 28243-28255.https://doi.org/10.1007/s11356-019-05945-x
Lokhande PB, Mujawar HA (2016) Graphic Interpretation and assessment of water quality in the Savitri River basin. Int J Sci & Eng Res 7(3): 1113-1123.
Meybeck M (1987) Global chemical weathering of surficial rocks estimated from river dissolved loads. Am J Sci 287(5): 401-428. https://doi.org/10.2475/ajs.287.5.401
Meybeck M, Ragu A (1997) River discharges to the oceans: an assessment of suspended solids, major ions, and nutrients. UNEP 243: 1-245.
Pant RR, Bishwakarma K, Qaiser FU, et al. (2021) Imprints of COVID-19 lockdown on the surface water quality of Bagmati river basin, Nepal. J Environ Manage 289(112522): 1-13. https://doi.org/10.1016/j.jenvman.2021.112522
Pant RR, Zhang F, Rehman FU, et al. (2018) Spatiotemporal variations of hydrogeochemistry and its controlling factors in the Gandaki River Basin, Central Himalaya Nepal. Sci Total Environ 622-623: 770-782.https://doi.org/10.1016/j.scitotenv.2017.12.063
Paudyal R, Kang S, Sharma CM, et al. (2016) Major ions and trace elements of two selected rivers near Everest region, southern Himalayas, Nepal. Environ Earth Sci 75(1): 1-11. https://doi.org/10.1007/s12665-015-4811-y
Piper (1944) A graphic producer in the geochemical interpretation of water-analysis. Eos, Trans Am Geophys Union 25(6): 914-928. https://doi.org/10.1029/TR025i006p00914
Qaisar FU, Zhang F, Pant RR, et al. (2018) Spatial variation, source identification, and quality assessment of surface water geochemical composition in the Indus River Basin, Pakistan. Environ Sci Pollut Res 25(13): 12749-12763. https://doi.org/10.1007/s11356-018-1519-z
Qu B, Zhang Y, Kang S, et al. (2019) Water quality in the Tibetan Plateau: major ions and trace elements in rivers of the “Water Tower of Asia”. Sci Total Environ 649(September): 571-581. https://doi.org/10.1016/j.scitotenv.2018.08.316
Raghunath HM (1987) Ground water: hydrogeology, ground water survey and pumping tests, rural water supply and irrigation systems. New Age Int. p 493.https://books.google.ca/books?hl=en&lr=&id=jdp0w5NVw-cC&oi=fnd&pg=PA1&dq=Raghunath+HM+(1987)+Ground+water:+hydrogeology,+ground+water+survey+and+pumping+tests,+rural+water+supply+and+irrigation+systems.+New+Age+Int.+p+493.&ots=sN-5ks6gbk&sig=c7N3l491faMcUzQLr9WN1CPEZ7A&redir_esc=y#v=onepage&q&f=false (Accessed on 12 September 2020)
Rai SK, Singh SK, Krishnaswami S (2010) Chemical weathering in the plain and peninsular sub-basins of the Ganga: Impact on major ion chemistry and elemental fluxes. Geochim Cosmochim Acta 74(8): 2340-2355.https://doi.org/10.1016/j.gca.2010.01.008
Richards LA (1954) Diagnostics and improvement of saline and alkaline soils. U.S. Dept. of Agric. p 69. https://books.google.com/books?hl=en&lr=&id=oivqg-Y_n8sC&oi=fnd&pg=PA17&dq=Richards+LA+(1954)+Diagnostics+and+improvement+of+saline+and+alkaline+soils.+U.S.+Dept.+of+Agric.+p+69.&ots=Ainm_qbWES&sig=POIyROfK34r12nmp8NgT9pugxXI (Accessed on 30 November 2020)
Rusydi AF (2018) Correlation between conductivity and total dissolved solid in various type of water: a review. IOP Confer Seri: Earth Environ Sci 118(1). https://doi.org/10.1088/1755-1315/118/1/012019
Salifu M, Aidoo F, Hayford MS, et al. (2017) Evaluating the suitability of groundwater for irrigational purposes in some selected districts of the upper west region of Ghana. Appl Water Sci 7(2): 653-662. https://doi.org/10.1007/s13201-015-0277-z
Sarin MM, Krishnaswami S, Dilli K, et al. (1989) Major ion chemistry of the Ganga-Brahmaputra river system: weathering processes and fluxes to the Bay of Bengal. Geochim Cosmochim Acta 53(5): 997-1009.https://doi.org/10.1016/0016-7037(89)90205-6
Sarin MM, Krishnaswami S, Trivedi JR, et al. (1992) Major ion chemistry of the Ganga source waters: weathering in the high altitude Himalaya. Proc Indian Acad Sci - Earth Planet Sci 101(1): 89-98. https://doi.org/10.1007/BF02839175
Seth R, Mohan M, Singh P, et al. (2016) Water quality evaluation of Himalayan Rivers of Kumaun region, Uttarakhand, India. Appl Water Sci 6(2): 137-147.https://doi.org/10.1007/s13201-014-0213-7
Sharif MU, Davis RK, Steele KF, et al. (2008) Inverse geochemical modeling of groundwater evolution with emphasis on arsenic in the Mississippi River Valley alluvial aquifer, Arkansas (USA). J Hydrol 350(1-2): 41-55.https://doi.org/10.1016/j.jhydrol.2007.11.027
Singh S, Ghosh NC, Gurjar S, et al. (2018) Index-based assessment of suitability of water quality for irrigation purpose under Indian conditions. Environ Monit Assess 190(1). https://doi.org/10.1007/s10661-017-6407-3
Stallard RF, Edmond JM (1983) Geochemistry of the Amazon 2: The influence of geology and weathering environment on the dissolved load. J Geophys Res 88(C14): 9671-9688. https://doi.org/10.1029/JC088iC14p09671
Subramanian V, Ramanathan AL (1996) Nature of sediment load in the Ganges-Brahmaputra river systems in India. Kluwer Acad Publ 151-168. https://doi.org/10.1007/978-94-015-8719-8_8
Thenkabail PS, Schull M, Turral H (2005) Ganges and Indus river basin land use/land cover (LULC) and irrigated area mapping using continuous streams of MODIS data. Remote Sens Environ 95(3): 317-341. https://doi.org/10.1016/j.rse.2004.12.018
Thomas J, Joseph S, & Thrivikramji KP (2015). Hydrochemical variations of a tropical mountain river system in a rain shadow region of the southern Western Ghats, Kerala, India. Appl Geochem 63:456-471.https://doi.org/10.1016/j.apgeochem.2015.03.018
Tsering T, Abdel-Wahed MSM, Iftekhar S, et al. (2019) Major ion chemistry of the Teesta River in Sikkim Himalaya, India: chemical weathering and assessment of water quality. J Hydrol: Region Stud 24(June): 100612.https://doi.org/10.1016/j.ejrh.2019.100612
Varol M, Gökot B, Bekleyen A, et al. (2013) Geochemistry of the Tigris River basin, Turkey: spatial and seasonal variations of major ion compositions and their controlling factors. Quat Int 304(August): 22-32.https://doi.org/10.1016/j.quaint.2012.12.043
Vass KK, Mondal SK, Samanta S, et al. (2010) The environment and fishery status of the River Ganges. Aquat Ecosyst Health Manag 13(4): 385-394.https://doi.org/10.1080/14634988.2010.530139
Walton NRG (1989) Electrical conductivity and total dissolved solids—what is their precise relationship? Desalination 72(3): 275-292. https://doi.org/10.1016/0011-9164(89)80012-8
WB (2010) Mapping the resilience of international river basins to future climate change-induced water variability. World Bank Water Sect 15: 1-75. https://doi.org/ISBN:978-960-6865-81-7
Yde JC, Riger-Kusk M, Christiansen HH, et al. (2008) Hydrochemical characteristics of bulk meltwater from an entire ablation season, Longyearbreen, Svalbard. J Glaciol 54(185): 259-272. https://doi.org/10.3189/002214308784886234
Zaman M, Shahid SA, Heng L (2018) Guideline for salinity assessment, mitigation and adaptation using nuclear and related techniques. Spring Nat. https://doi.org/10.1007/978-3-319-96190-3
Zhang J, Huang WW, Létolle R, et al. (1995) Major element chemistry of the Huanghe (Yellow River), China - weathering processes and chemical fluxes. J Hydrol 168(1-4): 173-203. https://doi.org/10.1016/0022-1694(94)02635-O